Future climate change will accelerate maize phenological development and increase yield in the Nemoral climate

R. Žydelis[1*], L. Weihermüller[2], M. Herbst[2]

[1]Institute of Agriculture, Lithuanian Research Centre for Agriculture and Forestry, Lithuania

[2]Agrosphere Institute (IBG-3), Forschungszentrum Jülich GmbH, Germany

[*] Corresponding author: Renaldas Žydelis, renaldas.zydelis@lammc.lt

Graphical abstract

Abstract

Climate change will bring warmer and wetter conditions and more frequent extreme events in the Nemoral climate zone. These changes are expected to affect maize growth and yields. In this study, we applied the AgroC model to assess climate change impact on changes in growing environmental conditions, growing season length, yield and potential yield losses due to multiple abiotic stresses. The model was calibrated and validated using data from dedicated field experiments conducted in Lithuania during four meteorologically contrasting years (2015, 2016, 2017 and 2019). We simulated the climate impacts on rainfed maize for long-term future climate conditions from 2020 to 2100 under the RCP2.6 (low), RCP4.5 (medium) and RCP8.5 (high) emission scenarios. As a result, we found that air temperature, sum of growing degree days and amount of precipitation during the growing season of maize will increase, especially under medium and higher emission scenarios (RCP4.5 and RCP8.5), with significantly positive effect on yields. The simulation results showed that average maize grain yield will increase under RCP2.6 by 69 kg ha^{-1} per decade, under RCP4.5 by 197 kg ha^{-1} per decade and under RCP8.5 by 304 kg ha^{-1} per decade. The future potential maize yield reveals a progressive increase with a surplus of +10.2% under RCP4.5 and +14.4% under RCP8.5, while under RCP2.6 the increase of potential yield during the same period will be statistically not significant. The yield gap under RCP2.6 and RCP4.5 will fluctuate within a rather narrow range and under RCP8.5, it will decrease.

Keywords: crop modelling, climate change, grain maize, yield potential

1. Introduction

Agricultural systems are inherently sensitive and vulnerable to climate fluctuations and the predicted future warming poses a substantial threat to crop production in many regions worldwide (IPCC, 2019). Rising temperatures, changing precipitation patterns, and higher frequency of droughts inducing crop water stress, as well as changes in frost, heat or cold stress have already impacted crop growth, development and yields (Ray et al., 2019). Climate variables can explain 20–49% of the variability of different crop yield anomalies on a global scale

(Vogel et al., 2019), whereby the strength of the climate change impact on crop production varies between regions and crops. Studies analysing climate change impacts from other factors (adapted management) influencing crop yields, have shown that, in many higher-latitude regions, yields of various crops (e.g. maize, sugar beet and wheat) were positively impacted throughout the last decades, while in many lower-latitude regions, the effects of climate change on specific crops (e.g. maize and wheat) was mostly negative in terms of yield (IPCC, 2019).

With future changing climate, the agricultural sector in the Nordic region can be either a winner or loser, and adaptation and management strategies for crop production will be one of the most important factors to avoid negative effects and to benefit from future climatic changes (Wiréhn, 2018). In general, the Nordic/Baltic region is characterised by rather high interannual variability in temperature and precipitation due to varying maritime, continental and Artic influences, depending on the large-scale circulation. Currently, air temperatures are below optimum level for maximum photosynthesis rates for many crops (e.g. maize, soybean) in the Nordic region. However, the region 60^0 North is one of the regions globally most affected by warming, with a significant increase of annual mean air temperature of 0.11 ^{0}C per decade over the period 1871−2011 (BACC Author Team, 2015) compared to a global mean air temperature increase of 0.06 ^{0}C per decade for the same period (IPCC, 2007). The study of Jaagus et al. (2014) provides data for the last six decades and they observed substantially increasing trends in maximum and minimum temperatures measured in spring (March and April) and in summer (July and August) for the Baltic countries. Additionally, for the next few decades, an even stronger increase in relation to the global mean temperature is predicted for the Nordic/Baltic region (BACC Author Team, 2015). Annual precipitation had increased in Northern Europe and decreased in Southern Europe (Kjellström et al., 2011). However, in-season precipitation distribution is much more important for plant growth and development. Jaagus et al. (2018) report that, for the period 1966−2015, monthly precipitation already increased during the winter season by about 10 mm per decade in Baltic countries. Precipitation variability during summer increased in frequency and intensity of extreme events also increased, leading to waterlogging, droughts and water shortages. Even though the forecasted warmer and wetter growing conditions are generally expected to be beneficial for Northern Europe, more frequent extreme weather events (e.g. heavy rains, summer droughts) pose a challenge for crop production (Kovats et al., 2014).

Maize (*Zea mays L.*) is a warm season C4 plant and has a specialised physiology with Kranz anatomy, which makes it well suited for warm and dry climates. However, extensive breeding interventions have made this crop appropriate for colder regions as well (Chaudhary et al., 2014). Maize growing mainly spans between 58° N to 40° S, from below sea level to altitudes higher than 3000 m and in areas with 250 to more than 5000 mm of annual rainfall (Dowswell et al., 1996). Maize is one of the top crops for human food, animal feed and biofuel production. Maize production must double to meet the growing world demand in the future (Meng et al., 2016). Globally, rainfed maize yields will be negatively impacted by a global warming of 0.5 ^{0}C (Schleussner et al., 2018). Future climate scenarios predict a loss of climatically suitable areas for maize cultivation in Central and

South America and Sub-Saharan Africa. In contrast, currently cooler regions such as Northern Europe and North America benefit from climate change for maize growing and could turn from suitable to optimal areas for maize cultivation (Ramirez-Cabral et al., 2017). In addition, Elsgaard et al. (2012) estimated that the maize cultivation fraction of the total agricultural area in Denmark, Sweden, Finland and the Baltic countries will increase by 4% to an overall 20% until 2040.

In general, maize grain yield in higher-latitude regions is significantly lower than the potential yield. A recent study has shown that in the Nemoral climate zone, potential maize grain yield can achieve about 11 t ha^{-1}, whereby yield losses due to abiotic stress factors are in the range of 3.2 t ha^{-1} (Žydelis et al., 2018). Abiotic stress factors adversely affect growth and development as well as productivity and cause many physiological, morphological and biochemical changes in plants (Sanghera et al., 2011). Currently, cold stress remains the dominant environmental factor for potential yield loss in the Nemoral climate zone, while the impact of water stress is of secondary importance for maize growth and development (Olesen et al., 2011). The projected impact of future climate change on potential maize yields and yield gap has not yet been adequately addressed in the Nemoral climate zone. However, a comprehensive climate change assessment could provide valuable information to farmers/growers or policymakers on the optimum adaptation strategy and how to mitigate the impact of climate change.

Traditional controlled environment and field experiments are restricted in analysing the effects of climate change on crops due to a relatively large number of possible combinations of temperature, precipitation, solar radiation and atmospheric CO_2. Crop models are, on the other hand, a valuable tool to assess the crop response to climate change, overcoming the constraints of field experiments. However, most current generation crop models were primarily calibrated and used to predict average climate conditions based on long-term climate data (Reichstein et al., 2013), and their algorithms simulating abiotic and biotic stresses are not sufficiently parameterised due to a lack of supplementing experimental field data. Nevertheless, if field experiments carried out under contrasting climatic conditions are used in combination with crop models, this could potentially contribute to understanding mechanisms of multiple and confounding stress factors under future climate conditions (Rötter et al., 2018).

The evolution of future climate is uncertain because of two main uncertainties in greenhouse gas emissions: (i) the financial and political turn of events; and (ii) a lack of information and understanding of the behaviour of the global climate system (Webber et al., 2020). Nevertheless, in recent years, the anticipated impact of future climate change on maize has been investigated (Araya et al., 2015; Ureta et al., 2020; Xiao et al., 2020). However, most of these studies have been conducted in areas where the current climate is suitable for maize cultivation and there remains a lack of studies in marginal climates. Besides, the majority of previous model studies used fixed planting days with a limited number of general circulation models (GCMs) and limited climate

information (growing degree days, temperature and precipitation changes) during the maize growth and development period.

In this study, we calibrated and validated the AgroC model using a comprehensive multiyear grain maize experiment with contrasting climatic conditions (2015 − cool and dry; 2016 − warm and wet; 2017− cool and wet; 2019 – warm and average precipitation) and provide a climate change impact assessment on maize yields using a plenteous number of GCMs and regional climate models (RCMs) under three representative CO_2 concentration pathways (RCPs); RCP2.6, RCP4.5 and RCP8.5 in Nemoral climate conditions. The objectives of this study were as follow: (1) to quantify the effect of a warming climate on meteorological variables during the maize growing period; (2) to disentangle the impacts of the individual climatic variables on maize yield; and (3) to estimate maize yield potential and to disentangle and quantify the confounding impact of cold and water stress under future climate conditions

2. Materials and methods

2.1. Study site

According to the environmental stratification of Europe, Lithuania is in the Nemoral climate zone, characterised as continental and cool with a rather short vegetation period. The southern part of Scandinavia, the Baltic states and Belarus are also attributed to this climate zone (Metzger et al., 2012). The territory of Lithuania is non-uniform in terms of air and soil temperature, precipitation distribution and soils. The average annual air temperature varies between 5.8–7.6 ^{0}C, and annual precipitation between 550–910 mm. The main soils are Luvisols, Cambisols, Gleysols, and Arenosols and cover 28.5, 15.9, 14.6 and 13.2% of the area, respectively. Field experiments with grain maize were conducted for four years at the Lithuanian Research Centre for Agriculture and Forestry located in Akademija (55° 39’ N, 23° 86’ E). Field experiment locations fall into the agro-climatic zone IID of central Lithuania (Bukantis, 2009), which is warm, relatively dry and typical for intensive cash crop production in Lithuania (see Fig. 1). The typical growing season starts in May and lasts until mid-October, the average temperature during the maize growing season is 13.9 ^{0}C (mean values over the period 1981−2010). The sum of growing degree days exceeds the Lithuanian average but according to soil water resources during the growing season, this zone is the driest in Lithuania and the seasonal (May−October) average precipitation is only 335.7 mm (mean value over the period 1981−2010).

2.2. Experimental layout

The maize early-season variety, AGIRAXX (characterised as FAO 190), was sown at a density of 7 plants m^{-2} (70,000 plants ha^{-1}; 0.75 m row spacing; 0.18 m plant spacing) at 6−8 cm depth in 2015−2017 and 2019 when the soil temperature in each year reached 8–10^o C. This variety was bred in France by RAGT Seed Company (Saffron Walden, UK). It was chosen because of its early maturity and suitability for growth in this region.

Fertilisers were applied manually and incorporated into the soil before maize seeding. Weeds were controlled using the herbicide MAISTER OD (rate 1.7 l ha^{-1}). Maize harvesting was performed manually after the first autumn frosts. The experimental design included ten treatments with different nitrogen sources and fertiliser levels. In this study, where water and cold stresses were investigated, we focused on the plots which were fertilised with ammonium nitrate (170 kg N ha^{-1}) and an additional mineral supply of superphosphate (90 kg ha^{-1} of P_2O_5) and potassium chloride (170 kg ha^{-1} of K_2O), to ensure optimal growth and development conditions. A randomised complete block design with four replicates was used, each with an experimental plot size of 30 m^2 (10 m length × 3 m width), whereby the inner part of the plots of 12 m^2 (8 m length × 1.5 m width) were harvested. The soil is classified as a Hypocalcic Stagnic Luvisol (Loamic, Drainic) (WRB, 2014). The main soil characteristics and management are presented in Table 1.

2.3. Plant and soil data collection as input, calibration and validation data for AgroC

During the maize vegetation period, plant development stages were frequently recorded. Maize vegetative and reproductive development stages were identified on the basis of the entire treatment when 50% or more of the plants were at a particular development stage. The leaf-collar method (Ritchie et al., 1986) was used for the development of vegetation stages, whereas reproductive stages were based on established visual indicators of kernel development.

Maize total above-ground biomass (TAB) was sampled five times per growing season at vegetative leaf stages 8 and 14 (growth stages V8 and V14), at the reproductive tasselling/silking and milking stages (growth stages VT/R1 and R3) and at physiological maturity (growth stage R6). In total, 20 randomly selected plants from each treatment (five per replicate) were cut at the soil surface and separated into the main components (if present at the sampling date): leaf (leaf blades), stem (stem and leaf sheaths), storage organs (cob, husk and tassel) and grain. The individual maize components were weighed (fresh mass) and dried at 65 ± 5 °C to a constant weight (dry weight). At the R6 growth stage, when more than 50% of the plants showed a visible black layer at the base of the kernel, two central rows of each plot from an area of 8 × 1.5 = 12 m^2 were cut to identify final TAB and grain yield. As in periodic biomass measurements, samples were taken from all replicates and oven-dried at 65 ± 5 °C until a fixed weight to receive dry TAB and yield weight.

Leaf area was measured five times per season (growth stages: V8, V14, VT/R1, R3, and R6), using a CL 203 Handheld Leaf Area metre (CID® Inc, WA, USA); based on these results, the leaf area index (LAI) was calculated.

For years 2015−2017 and 2019, the soil nutrient status was assessed for the arable soil layer (0−20 cm) from composite soil samples taken from 12 different locations within the experiment field. Soil pH, humus content, total nitrogen (N_{total}), plant-available phosphorus (P_2O_5) and potassium (K_2O) were analysed. Additionally, soil samples were taken from 0−30 and 0−60 cm depths for nitrate and ammonium content.

The soil hydraulic characteristics were measured in May 2017 using the HYPROP® (Meter Group, München, Germany) method as described by Schindler et al. (2010) in combination with the WP4® Dewpoint Potentiometer (Decagon Devices, WA, USA). Saturated hydraulic conductivity, K_{sat}, was measured using a falling head by the KSAT system (Meter Group, München, Germany). For all measurements, ten undisturbed soil samples of 250 cm^3 were extracted from the major soil horizons at depths of 15–20, 40–45, 70–75, 90–95, and 120–125 cm. Soil physical properties are summarised in Table 2.

In the years 2015−2017, the volumetric soil water content (SWC) was measured regularly (11 measurements in 2015 and 2017, eight measurements in 2016) at 0−10 cm soil depth using a portable TRIME-FM2 TDR system (IMKO, GmbH, Ettlingen, Germany). In addition, SWC was determined on site using site-specific calibrated 'Watermark' soil moisture sensors (Irrometer Company, Riverside, CA, USA) installed at 30 and 60 cm depth and replicated every 7−14 days.

2.4. AgroC model and parameterisation

The agroecosystem model, AgroC, is a mechanistic model for simulating the one-dimensional flux of soil water, soil heat, carbon turnover and crop growth in agricultural systems. A description of the model can be found in Herbst et al. (2008) and Klosterhalfen et al. (2017). For the estimation of crop phenological development (DVS) a normalized time scale, which is proportional to the temperature sum, is used. The development stage DVS is assumed to equal 1 at plant fluorescence. At crop maturity, the DVS value is 2. The increase in DVS on a daily basis over the growing season is estimated based on a temperature-dependent development rate by:

$$DVS_i = DVS_{i\text{-}1} + k_{DVS,I}(T_i) \quad \text{(Eq. 1)}$$

where $DVS_{t\text{-}1}$ represents DVS at the last timestep and $k_{DVS,i}$ is the development rate of DVS at the current timestep *i*, which is interpolated from two tables, one for DVS ≤ 1.0 and another one for DVS > 1.0, in dependence of daily average temperature *T*. Thus, lower development rates, usually observed after fluorescence, can be simulated. The two tables contain a number of temperature/k_{DVS} pairs and a linear interpolation is used to calculate k_{DVS} for the given temperature. The values of both tables are summarized in Supplementary Table 1.

In this study, the AgroC model was firstly run for four years (2015−2017 and 2019) using already calibrated maize (growth, morphology and phenology) and soil (hydraulic properties) parameters. The calibration procedure is discussed in Žydelis et al. (2018). In 2017, the simulated results showed a rather high TAB discrepancy between the measured and simulated values; thus, additional maize experimental data gathered in 2017 and in 2019 were used to recalibrate the AgroC crop parameters: 1 parameter = DVS (development stage) against fraction of dry matter allocated to the shoot; 2 parameter = DVS against reduction factor of maximal light assimilation rate; 3 parameter = mean temperature against reduction factor of maximal light assimilation rate,

which are responsible for maize growth and development. The recalibrated plant parameters used in the simulation of future maize yields are shown in Table S1. Data from the experimental plots in 2015 (cool and dry) and 2016 (warm and wet) were considered for model calibration and information from 2017 (cool and wet) and 2019 (warm and normal precipitation) growing seasons were used for model validation. For calibration and validation, measured experimental data of TAB partitioning (leaf, stem, storage organ weights, grain yield), LAI and SWC measured at 10, 30 and 60 cm depth were used.

2.5. Climate data and climate change scenarios

Daily weather records from 2015 to 2019, including maximum (T_{max}), minimum (T_{min}) and average (T_{avg}) temperatures (^{0}C), precipitation (P, mm), relative humidity (%), wind speed at 2 m height (m s^{-1}) and actual duration of daily sunshine (hours) were collected from the Dotnuva meteorological station of the Lithuanian Hydrometeorological Service (Ministry of Environment) located ~500 m from the maize experimental field (55° 39' N, 23° 86' E, at 66.45 m elevation). Reference Penman–Monteith evapotranspiration ($ET_{0,}$) (mm day^{-1}) was calculated according to Allen et al. (1998). The sum of heat units accumulated during a day (growing degree days, GDD), expressed in ^{0}C was calculated by subtracting the base temperature (8^0C) from the average air temperature.

For twenty-first century future climate projections, weather data from the H2020 European long-term ecosystem and socio-ecological research infrastructure project (eLTER, 2020), which provides climate scenario data based on an ensemble of RCM simulations (Table S2), were used. Time series were extracted from an ensemble of EURO-CORDEX RCM simulations. Three different representative concentration pathways (RCPs) of optimistic RCP2.6 (global mean atmosphere temperature below 2 ^{0}C), medium RCP4.5, and more pessimistic RCP8.5 emission scenarios were used for the period 2020−2100. For each RCP scenario, daily data of eight meteorological variables were retrieved and used to predict future maize yield.

The data was processed with the Climate DataOperator (CDO, 2020) v1.9.1, established by the Max Planck Institute for Meteorology (Max Planck Institute for Meteorology, 2020). The global atmospheric data were downscaled by using the information of 4 close by located weather stations, as described in more detail by Rennie et al. (2021). No further bias adjustment was applied to the downscaled time series, although this may represent a limitation (Hoffmann et al., 2018). A first reason for not doing so was the necessity to obtain suitable reference observations (Casanueva et al., 2020), a task that is far from being obvious given the large uncertainty in observational data sets (Kotlarski et al.,2018; Herrera et al., 2019; Prein and Gobiet, 2017). A second reason was the spatial resolution mismatch between gridded climate data and point-scale weather stations. Finally, no correction was needed to account for a possible difference in altitude between grid point and station data since this test site is located just above sea level and also close to the coastline.

2.6. Scenario settings

The maize growing period was analysed using simulated data from planting to physiological maturity. To evaluate the effect of climatic variables on potential maize yield and yield gap, the simulations were run for each climate prediction (local downscaled) for the individual RCP scenarios. As future maize seeding dates were unknown, sowing dates for the three RCP scenarios were calculated based on air temperature information, as air temperature is a good indicator (especially in cool climates) to predict feasible germination and eventual emergence (Abendroth et al., 2011). To do so, a suitable sowing date was searched in the period between 1 March to 1 June, whereby the seeding date was set to the first occurrence of a daily minimum air temperature in a period of four days of at least 10.0 ^{0}C. Projected maize sowing date shifts used in the simulations of future climate under different RCP scenarios are shown in Figure S1.

The effects of environmental limitations on maize yield were assessed as follows. In a first step, we calculated potential yield switching off plant responses to temperature and water (no abiotic stresses) and assuming optimal fertilization. In a second step, we turned off only the function describing temperature. This allowed calculating water-limited yields. In a third step, we repeated the procedure for evaluating temperature-limited yields, turning off this time the function describing water stress. Finally, we simulated actual maize yields turning on both response functions. The difference between potential yields and the yields obtained in steps two to four provides a measure of the yield gaps arising from cold temperature, water stress and both stressors combined.

In total, 99 simulation runs were performed including different climate models, three RCPs and yield gap analysis.

2.7. Statistical analysis

Linear correlation-regression analyses were performed to estimate the relationships between climatic variables and maize yield. The statistical significance levels considered were: 'ns' to indicate no significance ($p >$ 0.05); '*' to indicate $0.05 \geq p > 0.01$; '**' to indicate $0.01 \geq p > 0.001$; and '***' to indicate $p \leq 0.001$. The coefficient of variation was calculated as the ratio of the standard deviation and mean. All statistical analyses were performed using SAS 9.4 (SAS Institute Inc., 2016).

3. Results and discussion

3.1. Model calibration and validation

The simulation results after calibrating the AgroC model for SWC for the three measurement depths, TAB and its partitioning, LAI as well as DVS are shown in Figure 2 and Table 3 along with the R^2 and root mean square error (RMSE). In general, the SWC for the three depth, TAB and its partitioning into grain yield, leaf, stem and storage organ biomass, as well as the LAI for the calibration period (2015–2016) were well represented. This also

holds for the validation period (2017 and 2019) for the crop parameters and SWC (2017). Note, that no field experiment was performed in 2018.

In more detail, the simulated temporal dynamics of the SWC for the upper soil layers during the calibration period (2015−2016) showed a fairly good agreement with an R^2 of 0.51 and RMSE of 0.039 cm^3 cm^{-3}. The agreement between simulated and observed SWC during the validation period (2017) was tolerable, with an R^2 of 0.49 and RMSE of 0.051 cm^3 cm^{-3}. The SWC dynamics measured at 30 cm depth were slightly better represented by the simulations compared to the 10 cm depth with R^2 values of 0.60 and lower RMSE values of 0.017 for the calibration period and an R^2 of 0.70 and RMSE of 0.021 cm^3 cm^{-3} for the validation period. During the calibration period, the observed SWC measured at 60 cm soil depth varied only in a narrow range during the maize growing season, while during the validation period, the SWC showed greater fluctuation and was closer to saturation. The statistical indicator, R^2 and RMSE indicated that during calibration and validation periods the model captured the pattern of SWC dynamics at 60 cm (Fig. 2) moderately well. The R^2 and RMSE values for the calibration period were 0.50 and 0.028 cm^3 cm^{-3}, respectively. For the validation period, the R^2 and RMSE values were quite similar to those for the calibration period, with an R^2 of 0.46 and RMSE of 0.032 cm^3 cm^{-3}.

Simulated TAB over the growing seasons was also captured reasonably well by the model. The statistical measures of the calibration period (2015−2016) indicated a good agreement between observed and simulated TAB with an R^2 and RMSE of 0.98 and 0.70 t ha^{-1}, respectively. These statistical measures were slightly lower for the validation period (2017 and 2019), with an R^2 of 0.98 and RMSE of 1.15 t ha^{-1}. A similar model performance was found for grain yield, where the predicted values confirmed those observed during the calibration period, with an R^2 of 0.98 and RMSE of 0.88 t ha^{-1}. The validation results for grain yield showed an R^2 of 0.98 and RMSE of 0.62 t ha^{-1}, indicating similar results in relation to the calibration. In general, grain yields varied substantially among the different years and yields were higher by ≈ 31.3% than the average yield reported by Lithuanian Farmers for the investigated years (Eurostat, 2020).

The ability of the AgroC model to simulate LAI is shown in Figure 2. Observed LAI varied between the years, but simulated LAI in some years overestimated the observations. The statistical measures were reasonably good during the calibration years with an R^2 of 0.97 and RMSE of 0.63. In the validation years, the R^2 for LAI was 0.92 while the RMSE was 0.99.

Simulated maize emergence, flowering, and harvest date differed by 2 to 4, 0 to 2, and 3 to 5 days from the observed date, respectively.

3.2. Projected changes in meteorological conditions during future maize growing seasons

In a first step, we analysed the projected future air temperature, the sum of growing degree day (GDD) and precipitation over the future maize growing season for the period 2020−2100 (Fig. 3). Therefore, we calculated the arithmetic mean and the standard deviation of the individual climatic variables of all downscaled projections

for each of the three individual RCPs (RCP2.6, RCP4.5 and RCP8.5). Based on the mean, a linear trend was calculated and is plotted in Figure 3. A clear warming and wetting trend under RCP4.5 and RCP8.5 was predicted, while for the RCP2.6, no clear trend could be found for the study region, neither for temperature nor for precipitation. For the mean temperature, the linear upward trends were ≈ 0.34 ^{0}C per decade, from 15.0 ^{0}C in the 2020s to 17.4 ^{0}C in the 2090s for RCP8.5, and ≈ 0.19 ^{0}C per decade, from 14.9 ^{0}C in the 2020s to 16.2 ^{0}C in the 2090s for RCP4.5. The predicted sum of GDD showed an even larger increase compared to the mean temperature of ≈ 60.0 ^{0}C per decade for RCP8.5, ≈ 27.0 ^{0}C per decade for RCP4.5 and only ≈ 2.9 ^{0}C per decade for RCP2.6. Projected changes in precipitation over the maize growth period indicated an increase of precipitation, whereby the precipitation was highly variable between years (Fig. 3). Nevertheless, precipitation increased ≈ 6.3 mm per decade from 394.2 mm in the 2020s to 438.2 mm in the 2090s for RCP8.5 and ≈ 4.2 mm per decade from 366.5 mm in the 2020s to 396.1 mm in the 2090s for RCP4.5. A slightly different picture can be seen for RCP2.6, where precipitation increased from 362.2 mm in the 2020s to 402.8 mm in the 2050s and decreased thereafter to 365.2 mm in the 2060s and increased again to 391.2 mm for the 2090s.

In general, the data show that air temperature, the sum of GDD and precipitation during the maize growing season will clearly increase in RCP4.5 and RCP8.5 scenarios, with the picture being less clear for the RCP2.6 scenario.

3.3. Climate change impact on maize growing season length

Based on the data presented above, the length of the maize growing season (sowing to physiological maturity taken from the simulation results) was calculated for the different decades and reveals a progressive decrease from 152 days in the 2020s to 145 days in the 2090s (−4.6%) for RCP2.6, from 151 days in the 2020s to 142 days in the 2090s (−5.9%) for RCP4.5 and from 149 days in the 2020s to 137 days in the 2090s (−8.1%) for RCP8.5. Generally, the maize growth period decreased more rapidly under RCP8.5 (−1.8 days per decade) compared to RCP4.5 (−1.4 days per decade) or RCP2.6 (−1 day per decade), indicating that larger changes in climatic conditions, as shown in Figure 3, will lead to shortened growth periods, which will lead to a possible increase of effective maize growing days i.e. days combining sufficient temperature and water availability. Currently, the low number of plant effective growing days is likely to be a rather significant limiting factor influencing modest yields in the Northern European regions (Peltonen-Sainio, 2012)

In a next step, the climate induced changes in maize phenology were estimated. Hereby, the vegetative (sowing−tasselling) and reproductive (silking−maturity) period lengths were highly relevant. The results showed that the maize vegetative period will gradually and significantly ($p < 0.05$) decrease under RCP4.5 and RCP8.5, with a decreasing trend of −0.62 and −0.37 days per decade for RCP8.5 and RCP4.5. On the other hand, the average maize vegetative period length under RCP2.6 will remain stable under future climate conditions (≈ 3

months ranging between 98−100 days). A similar declining trend was calculated for the maize reproductive (grain filling) period but reproductive period under all emissions scenario will shorten approximately twice as fast as the vegetative period with −0.68, −0.98, and −1.13 days per decade under RCP2.6, RCP4.5, and RCP8.5, respectively. Based on these data, more favourable growing conditions will likely promote the northward expansion of maize cultivation due to the stronger growth compared to other cereal plants.

3.4. Simulated future maize yields

AgroC simulated maize TAB showed a continuous and significant ($p < 0.05$) increasing trend under RCP4.5 and RCP8.5, with an increase of 354 and 315 kg ha^{-1} per decade for RCP8.5 and RCP4.5 under long-term future climate conditions (Fig. 5). The average TAB increase under RCP2.6 was not significant and reached approximately only half (190 kg ha^{-1} per decade) of the increase of the higher emission scenarios (RCP4.5 and 8.5). For grain yield, the 80-year linear upward trend indicated an increase rate of 304 and 197 kg ha^{-1} decade for RCP8.5 and RCP4.5, respectively, and only 69 kg ha^{-1} decade for RCP2.6, which is only ⅓ and ¼ of the increase was found for the higher emission scenarios. Improvements in maize harvest index (harvest index HI = ratio of TAB to GY) can be expected, especially under RCP8.5 scenario with an increase from 47.0 % in the 2020s to 51.0 % in the 2090s. A slight increase is also forecasted under RCP4.5 from 46.9 % in the 2020s to 48.8 % in the 2090s, while under RCP2.6 HI will remain constant and reach ~ 46.0 %. The coefficient of variation (CV) of the maize TAB, associated with interannual fluctuations, varied between 13.8−15.9% under RCP2.6, from 15.6 to 19.6% under RCP4.5, and from 13.8 to 16.9% under RCP8.5. Grain yields, on the other hand, generally showed slightly higher CV from 12.1 to 16.7% under RCP2.6, from 17.2 to 21.3% under RCP4.5, and from 16.3 to 21.2% under RCP8.5, respectively. The relatively large TAB and grain yield fluctuations within each year provide a good opportunity to analyse the effect of individual future weather variables on maize productivity.

The study of Iizumi et al. (2017) revealed that global maize yields, with limited warming (RCP2.6), will stagnate across 83% of the global growth area by the end of twenty-first century even if agronomic adjustments (field management systems, sowing date) are considered. The authors also stated that the maize yield stagnation will be even more severe under faster warming conditions (RCP4.5 and RCP6.0) and finally, will start to decrease under the pessimistic RCP8.5 scenario with the highest warming. In contrast, our study shows that climate change will have a positive effect on maize yield under the Nemoral climate, being one of the regions worldwide which will positively benefit from global warming with respect to increased maize yields.

3.5. Relations between climatic variables and maize grain yield

In order to find relations between the climatic variables and simulated future maize yields, linear regressions between mean air temperature, sum of GDD, precipitation over the growing period and grain yield

were established (see Fig. 6). A significant positive regression was found between mean temperature and grain yield, whereby the R^2 values were low for RCP2.6 at 0.19 and moderate for RCP4.5 and RCP8.5 at 0.42 and 0.63, respectively. The sum of GDD showed slightly higher regression coefficients for all RCP scenarios. This effect was strongest under RCP8.5 ($R^2 = 0.68$, $p < 0.001$), moderate under RCP4.5 ($R^2 = 0.52$, $p < 0.001$), while under RCP2.6, the GDD effect on maize yield was low ($R^2 = 0.27$, $p < 0.001$). Based on this, we can conclude, that GDD (amount of warmth available for plant growth) is the main climatic factor affecting positive maize grain yield changes in Nemoral climates. In contrast, the effects of precipitation changes were less pronounced in relation to the mean temperature and sum of GDD on maize yield with a non-significant regression under RCP2.6, low under RCP4.5 ($R^2 = 0.16$, $p < 0.05$) and RCP8.5 ($R^2 = 0.21$, $p < 0.001$).

3.6. Potential maize yields and yield gap

The predicted potential maize yield (without water and cold stress) showed a continuous and significant increase from 11.1 t ha^{-1} in the 2020s to 12.7 t ha^{-1} in the 2090s (+14.4%) for RCP8.5, and from 10.9 t ha^{-1} in the 2020s to 12.0 t ha^{-1} in the 2090s (+10.2%) for RCP4.5. Potential maize yield increase under RCP2.6 was not significant within narrow limits from 10.4 to 11.5 t ha^{-1} (see Fig. 7). In general, the projected increase of potential maize yields under RCP8.5 were slightly higher (0.23 t ha^{-1} per decade) than under RCP 4.5 (0.16 t ha^{-1} per decade), while for the RCP2.6, no clear trend for potential yield could be found.

According to the global yield gap atlas (www.yieldgap.org), the highest water-limited yield potential (90^{th} percentile; > 10.0 t ha^{-1}) of rainfed maize in Europe is estimated for Atlantic Central (Belgium – 12.6, Netherlands – 13.0 t ha^{-1}), Alpine South (Austria – 12.5, Switzerland – 12.7 t ha^{-1}), as well continental climate zones (Germany – 11.0, Poland – 11.0 t ha^{-1}) for the current climate. For irrigated maize, the highest yields in Europe were estimated for northern, southern and mountainous Mediterranean zones (Spain – 14.7, Portugal – 15.1, France – 14.6, Italy – 13.8 and Greece – 13.3 t ha^{-1}). According to our findings, by the end of the 21^{st} century, the potential maize yield will increase under Nemoral climate conditions. Considering climate change, maize can become a new, widely grown crop at latitudes > 60^0 in future due to on average more favourable growing conditions (warmer and wetter).

The simulated maize yield loss in individual years due to water stress varied from 0.14 to 2.64 t ha^{-1}, which equals a relative yield gap from 2.2 to 26.1% under RCP2.6, from 2.2 to 20.4% under RCP4.5 (0.16 to 2.17 t ha^{-1}), and 1.8 to 20.1% under RCP8.5 (0.14 to 2.77 t ha^{-1}). On the other hand, yield loss due to water stress showed a constant decrease from 1.0 t ha^{-1} (relative yield gap of 9.5%) in the 2020s to 0.8 t ha^{-1} per decade (8.4%) in the 2050s, and started to increase steadily to 1.5 t ha^{-1} per decade (13.0%) in the 2080s with a further decrease to 1.1 t ha^{-1} per decade (9.7%) for the 2090s under RCP2.6 (Fig. 7). Rather different trends prevailed under the RCP4.5 scenarios. Maize yield losses due to water shortage would increase from 0.7 t ha^{-1} per decade (6.7%) in the 2020s to 1.2 t ha^{-1} per decade (10.8%) in 2040s, then decrease to 0.6 t ha^{-1} per decade (5.4%) in the 2050s, and start to increase to 1.1 t ha^{-1} per decade (9.1%) in the 2080s, eventually decreasing again to 1.0 t ha^{-1} per decade (8.2%)

414 in the 2090s. A more severe trend in maize yield losses can be seen under RCP8.5 where two periods can be clearly
415 distinguished. From the 2020s to 2050s, yield losses due to water stress will increase from 0.7 t ha^{-1} per decade
416 (or 6.6%) to 1.4 t ha^{-1} per decade (or 11.1%), and decrease to 1.2 t ha^{-1} per decade (10.1%) in the 2060s before
417 constantly increasing to 1.5 t ha^{-1} per decade (12%) in the 2090s.
418 Although, projected changes in precipitation over the maize growth period indicated an increase of
419 precipitation under higher emission scenarios in RCP4.5 and RCP8.5 (Fig. 3), climate change will possibly
420 increase the variability and distribution (the yearly coefficient of variation will increase) of seasonal precipitation;
421 thus, increasing total precipitation will not necessarily be sufficient to supply the maize with water over the entire
422 growing period. For Europe, Schaldach et al. (2012) provided an overview of possible climate change effects on
423 agriculture and concluded that, in Northern Europe, the increase in air temperatures will increase potential
424 evapotranspiration, not assessing improved water use efficiency caused by elevated CO_2 concentrations, and may
425 lead to an increased water demand for irrigation for some crops including maize. Therefore, water stress will be a
426 significant abiotic factor limiting maize yields, even though the total amount of precipitation will probably increase
427 in future. In fact, the most critical period for maize growth is from tasselling to silking (VT−R1) and any stress,
428 especially water stress, during this period significantly reduces the kernel number per ear and also the kernel
429 weight (Abendroth et al., 2011). In contrast, water stress occurring during maize vegetative development stages
430 (VE−VT) significantly affects crop height, leaf size and weight (Çakir, 2004), while a water deficit during maize
431 maturation stages (R4−R6) directly reduces the grain filling rate (Zhang et al., 2019).
432 The simulated maize yield losses due to low temperature stress (= cold stress at temperatures < 8 ^{0}C)
433 varied from 1.2 to 3.9 t ha^{-1} (10.7–40.0%) under RCP2.6, from 1.8 to 3.8 t ha^{-1} (16.5–31.0%) under RCP4.5 and
434 from 1.1 to 3.6 t ha^{-1} (8.8–31.8%) under RCP8.5 (Fig. 7), respectively.
435 The simulated trend in grain yield losses due to low temperatures did not show the same temporal pattern
436 under different RCP scenarios. For the RCP2.6 scenario, two periods of cold stress can be distinguished. One from
437 the 2020s to the 2040s, where the yield losses due to cold stress varied in a rather narrow range with on average
438 2.4–2.7 t ha^{-1} per decade (22.8−24.6% yield gap), and a second period (2050s to 2090s), where the cold stress
439 would cause slightly lower maize yield losses varying from 2.3 to 2.5 t ha^{-1} per decade or 20.8−23.4%. A slightly
440 different trend can be observed under RCP4.5, where the yield losses due to low temperatures in the future three
441 decades will fluctuate in a range from 2.6 to 3.1 t ha^{-1} per decade (22.9−26.9%), whereby the yield losses will
442 progressively decrease from 2.7 t ha^{-1} (25.5%) in 2050s to 2.3 t ha^{-1} (19.0%) in 2090s. In contrast, a different
443 picture can be seen for RCP8.5, where yield losses steadily decreased for every decade from 3.0 t ha^{-1} per decade
444 (26.9%) in the 2020s to 1.6 t ha^{-1} per decade (12.7%) in the 2090s. In conclusion, the results showed that yield
445 losses due to low temperatures simulated under the RCP4.5 and RCP8.5 scenarios are expected to decrease in the
446 mid and long-term future (2050−2090s), whereby it is likely that this decrease will be caused by the projected
447 changes in the length of the decadal maize growing season.

Water and cold stress are among the two most important environmental factors affecting maize growth, development and yield developing processes under a Nemoral climate. Currently, the main climatic limitation of maize growth in Nemoral regions is the growing season length, occurrence of late and early frosts, low soil water conditions during the growing season and associated droughts (Olesen et al., 2011). Although, the effect of water and cold stress on maize growth has been widely studied individually (e.g. Riva-Roveda et al., 2016; Sah et al., 2020), little is known about their combined effect on maize yield losses under future climate conditions in the Nemoral climate zone. Under natural field conditions, multiple stress factors often occur in combination, and therefore, we analysed how much maize yield losses can be expected when both stress factors occur in combination.

The simulated maize yield losses due to combined water and cold stress varied from 2.2 to 6.3 t ha^{-1} (15.9–53.6%) under RCP2.6, from 2.1 to 4.9 t ha^{-1} (21.5–39.1%) under RCP4.5 and from 1.9 to 5.1 t ha^{-1} (18.3–39.3%) under RCP8.5.

When analysing maize yield losses as a result of combined water and cold stress for the RCP2.6 scenario, two periods can be distinguished. During the first period, i.e. from the 2020s to the 2050s, yield losses consistently decreased from 3.7 t ha^{-1} to 3.2 t ha^{-1}. During the second period, i.e. from the 2060s to the 2090s, the average decade yield losses were slightly higher and fluctuated from 3.2 to 3.9 t ha^{-1}. Under the RCP4.5 scenario, yield losses during the next five decades (2020−2060s) will fluctuate in the range of 3.3 to 4.0 ha^{-1} (or 30.9–34.4%) and then slightly decrease in the long-term future (2070–2090s) and will range from 3.3 to 3.6 t ha^{-1} (27.1–29.5%). Despite the fact that the potential maize yield under RCP8.5 showed a continuous increase, the yield losses in the next eight decades will be similar and will fluctuate in the range of 3.1 to 4.0 t ha^{-1}, while the relative yield gap under the RCP8.5 scenario will steadily decrease from 33.5% in the 2020s to 24.7% in the 2090s. Schils et al. (2018) analysed cereal yield gaps across Europe and found that the yield gap of rainfed maize can reach up to 8.9 t ha^{-1}, or up to 75%. They also concluded that, in Western Europe, the relative yield gap is below 30%, while in Eastern Europe, the yield gap is slightly higher and reaches more than 40%. The study of Liu et al. (2017) found that, in all of China, the rainfed maize yield gap is ≈ 35%, while in different regions the yield gap may range from ≈ 15 to 47% (Northeast China – 35%, Northwest China – 15%, North China Plain – 31% and Southwest China – 47%).

4. Summary and conclusions

In the present study, the agroecosystem model, AgroC, was used and driven by local downscaled climate data from different GCMs for the next 80 years under RCP2.6, RCP4.5 and RCP8.5 emission scenarios to assess the impacts of climate change on rainfed maize production in the Nemoral climate conditions of Lithuania. Previously, the model was calibrated and validated using multiyear field experiments under contrasting weather conditions. By analysing the long-term future climate conditions for this region, it was found that the air

temperatures, the sum of GDD and the amount of precipitation will increase, particularly under the higher emission scenarios (RCP4.5 and RCP8.5) during the maize growing period, which will generate warmer and wetter environmental conditions for maize growth. The projected more favourable environmental conditions will primarily result in increasing number of effective growing days, which will have a positive effect on grain yields.

The simulation results verified this assumption, as the average maize grain yield will increase under RCP8.5 by 304 kg ha^{-1} per decade and under RCP4.5 by 197 kg ha^{-1} per decade. The smallest emission scenario (RCP2.6) indicated a lesser increase of only 69 kg ha^{-1} decade. Additionally, the potential maize yields and yield gaps were calculated. Under RCP4.5 and RCP8.5, the potential yield reveals a progressive increase in future with a surplus of +10.2% (2020s – 10.9 t ha^{-1}; 2090s −12.0 t ha^{-1}) under RCP4.5 and +14.4% (2020s – 11.1 t ha^{-1}; 2090s – 12.7 t ha^{-1}) under RCP8.5, while under RCP2.6, the increase of potential yield during the same period will be statistically not significant. The simulated yield losses due to water and temperature stress for the 2020−2100 period showed a wide range and varied from 15.9 to 53.6% under RCP2.6, from 21.5 to 39.1% under RCP4.5 and from 18.3 to 39.3% under RCP8.5. In summary, our results suggest that while potential yields could significantly increase in future, yield gaps would remain at similar levels as found under present climatic conditions or even decrease.

In our study, we demonstrated that, in the short, mid and long-term future, projected climate change in the Nemoral climate zone will generate favourable conditions for maize growth, i.e. maize yields and yield potential will steadily increase, while the yield gap will remain constant or even decrease slightly. These maize-friendly growing conditions, together with agronomic adjustments (longer season varieties, adjusted sowing time), agricultural policy and market conditions could trigger a significant increase in maize cultivation at the expense of other crops. In another study, Parent et al. (2018) concluded that by 2050 climate change could have positive impacts on maize yields in Europe based on the assumption that farmers will use optimal practices, i.e. adapting plant cycle duration and sowing dates to the diversity of environmental conditions. Whether the assumption will effectively be put in practice remains to be seen, but the results of our study certainly provides a motivation for farmers to adopt maize as a main crop also in the Nemoral climate zone of Lithuania.

Acknowledgements

The internship (02/11/2019−04/12/2019) at the Agrosphere Institute IBG-3 at the Forschungszentrum Juelich, Germany was funded by EU Structural Funds under Measure No. 09.3.3-LMT-K-712 ‘Development of scientific competence researchers, other researchers, students through practical scientific activities’ under a grant agreement with the Research Council of Lithuania (LMTLT). This research was partially funded by the Deutsche Forschungsgemeinschaft (DFG, German Research Foundation) under Germany’s Excellence Strategy - EXC 2070 – 390732324.

518 **References**
519

520 Abendroth L.J., Elmore R.W., Boyer M.J., Marley S.K. 2011. Corn growth and development. PMR 1009. Iowa
521 State University. Extension and Outreach, Ames. Iowa, USA.
522 Allen RG, Pereira LS, Raes D, Smith M. 1998. Crop evapotranspiration: Guidelines for computing crop
523 requirements. Irrigation and Drainage Paper No. 56, FAO, Rome, Italy.
524 Araya A., Hoogenboom G., Luedeling E., Hadgu K.M., Kisekka I., Martorano L.G. Assessment of maize growth
525 and yield using crop models under present and future climate in southwestern Ethiopia. Agricultural Forest
526 Meteorology, 214−215, 252−265. doi.org/10.1016/j.agrformet.2015.08.259
527 BACC II Author Team. 2015. Second Assessment of Climate Change for the Baltic Sea Basin. Springer, 83.
528 doi.org/10.1007/978-3-319-16006-1
529 Bukantis, A. 2009. Agroclimatic zoning. Lithuanian National Atlas. Vilnius: National Land Service under the
530 Ministry of Agriculture.
531 Çakir R. 2004. Effect of water stress at different development stages on vegetative and reproductive growth of
532 corn. Field Crops Research, 89 (1): 1−16. doi.org/10.1016/j.fcr.2004.01.005
533 Casanueva A., Herrera S., Iturbide M., Lange S., Jury M., Dosio A., Maraun D., Gutiérrez J. M. 2020. Testing
534 bias adjustment methods for regional climate change applications under observational uncertainty and
535 resolution mismatch. Atmospheric Science Letters, 21, e978. doi.org/10.1002/asl.978
536 Chaudhary D.P., Kumar S., Langyan S. 2014. Maize: nutrition dynamics and novel uses. In Anand A, Khetarpal
537 S, Singh MP (eds). Physiological Response of Maize under Rising Atmospheric CO2 and temperature.
538 Springer, India, pp. 105−115. https://doi.org/10.1007/978-81-322-1623-0_9
539 Dowswell CR, Paliwal RL, Cantrell RP (1996) Maize in the third world. Wastvier Press, Boulder, pp. 268
540 Elsgaard L., Børgesen C.D., Olesen J.E., Siebert S., Ewert F., Peltonen-Sainio P., Rötter R.P., Skjelvåg A.O. 2012.
541 Shifts in comparative advantages for maize, oat and wheat cropping under climate change in Europe. Food
542 additives and Contaminants: Part A 29 (10): 1514−1526. doi.org/10.1080/19440049.2012.700953
543 eLTER. 2020. http://www.lter-europe.net/elter (2020), Accessed 1st Nov 2020.
544 Eurostat. 2020. Crop production in EU standard humidity. Available at:
545 https://ec.europa.eu/eurostat/databrowser/view/APRO_CPSH1__custom_58016/default/table?lang=en
546 Herbst M., Hellebrand H.J., Bauer J., Huisman J.A., Šimůnek J., Weihermüller L., Graf A., Vanderborght J.,
547 Vereecken H. 2008. Multiyear heterotrophic soil respiration: Evaluation of a coupled CO_2 transport and carbon
548 turnover model. Ecological Modelling, 214 (2−4): 271−283. doi.org/10.1016/j.ecolmodel.2008.02.007
549 Herrera S., Kotlarski S., Soares P. M. M., Cardoso R. M., Jaczewski A., Gutiérrez J. M., and Maraun, D. 2018.
550 Uncertainty in gridded precipitation products: Influence of station density, interpolation method and grid
551 resolution. International Journal of Climatology, 39: 3717–3729. doi.org/10.1002/joc.5878

552 Hoffmann P., Menz C., Spekat A. 2018. Bias adjustment for threshold-based climate indicators. Advance in Science
553 and Research, 15: 107–116. doi.org/10.5194/asr-15-107-2018
554 Iizumi T., Furuya J., Shen Z., Kim W., Okada M., Fujimori S., Hasegawa T., Nishimori M. 2017. Responses of crop
555 yield growth to global temperature and socioeconomic changes. Scientific Reports, 7: 7800.
556 doi.org/10.1038/s41598-017-08214-4
557 IPCC 2007. In: Solomon S, Qin D, Manning M, Chen Z, Marquis M, Averyt K.B. Tignor M, Miller HL (eds).
558 Climate change 2007: the physical science basis. Contribution of Working Group I to the Fourth Assessment
559 Report of the Intergovernmental Panel on Climate Change. Cambridge University Press, Cambridge.
560 IPCC, 2019: Summary for Policymakers. In: Climate Change and Land: an IPCC special report on climate change,
561 desertification, land degradation, sustainable land management, food security, and greenhouse gas fluxes in
562 terrestrial ecosystems [P.R. Shukla, J. Skea, E. Calvo Buendia, V. Masson-Delmotte, H.- O. Pörtner, D. C.
563 Roberts, P. Zhai, R. Slade, S. Connors, R. van Diemen, M. Ferrat, E. Haughey, S. Luz, S. Neogi, M. Pathak,
564 J. Petzold, J. Portugal Pereira, P. Vyas, E. Huntley, K. Kissick, M. Belkacemi, J. Malley, (eds.)]. In press.
565 Jaagus J, Briede A, Rimkus E, Sepp M. 2018. Changes in precipitation regime in the Baltic countries in
566 1966−2015. Theoretical Applied Climatology, 131: 433−443. DOI: 10.1007/s00704-016-1990-8
567 Jaagus J, Briede A, Rimkus E, Remm K. 2014. Variability and trends in daily minimum and maximum
568 temperatures and in the diurnal temperature range in Lithuania, Latvia and Estonia in 1951−2010. Theoretical
569 Applied Climatology, 118: 57−68. DOI: 10.1007/s00704-013-1041-7
570 Kjellström, E, Nikulin G, Hansson U, Strandberg G and Ullerstig A. 2011. 21st century changes in the European
571 climate: uncertainties derived from an ensemble of regional climate model simulations. Tellus, 63A: 24−40.
572 doi.org/10.1111/j.1600-0870.2010.00475.x
573 Klosterhalfen A., Herbst M., Weihermüller L., Graf A., Schmidt M., Stadler A., Schneider K., Subke J.A.,
574 Huisman J., Vereecken H. 2017. Multi-site calibration and validation of a net ecosystem carbon exchange
575 model for croplands. Ecological Modelling, 363: 137−156. doi.org/10.1016/j.ecolmodel.2017.07.028
576 Kotlarski S., Szabó P., Herrera S., Räty O., Keuler K., Soares P. M., Cardoso R. M., Bosshard T., Pagé C., Boberg
577 F.,Gutiérrez J. M., Isotta F. A., Jaczewski A., Kreienkamp F.,Liniger M. A., Lussana C., Pianko-Kluczynska,
578 K. 2017. Observational uncertainty and regional climate model evaluation: a pan-European perspective.
579 International Journal of Climatology, 39: 3730–3749. doi.org/10.1002/joc.5249
580 Kovats R.S., Valentini L.M., Bouwer E., Georgopoulou D., Jacob E., Martin M., Rounsevell, Soussana J.F. 2014.
581 Europe. In: Climate change 2014: Impacts, Adaptation, and vulnerability. Part B: Regional Aspects.
582 Contribution of Working Group II to the Fifth Assessment Report of the Intergovernmental Panel on Climate
583 change [Barros V.R., Field C.B., Dokken D.J., Mastrandrea M.D., Mach K.J., Bilir T.E., Chatterjee M., Ebi
584 K.L., Estrada Y.O., Genova R.C., Girma B., Kissel E.S., Levy A.N., MacCracken S., Mastrandrea P.R., White

585 L.L. (Eds). Cambridge University Press, Cambridge, United Kingdom and New York, NY, USA, pp 1267–
586 1326.
587 Liu B., Chen X., Meng Q., Yang H., Wart J. 2017. Estimating maize yield potential and yield gap with agro-
588 climatic zones in China – Distinguish irrigated and rainfed conditions. Agricultural and Forest Meteorology,
589 239:108−117. doi.org/10.1016/j.agrformet.2017.02.035
590 Maraun D. 20116. Bias Correcting Climate Change Simulations – a Critical Review. Current Climate Change
591 Reports, 2:211–220. doi.org/10.1007/s40641-016-0050-x
592 Max Planck Institute for Meteorology: available at: https://www.mpimet.mpg.de/en/home, last access: 1 August
593 2020
594 Meng Q., Chen X., Lobell D. B., Cui Z., Zhang Y., Yang H., Zhang. 2016. Growing sensitivity of maize to water
595 scarcity under climate change. Scientific reports, 6, 19605. https://doi.org/10.1038/srep19605
596 Metzger M.J., Shkaruba A.D., Jongman R.H.G., Bunce R.G.H. 2012. Description of the European environmental
597 zones and strata. Alterra Report 2281. Wageningen.
598 Olesen JE, Trnka M, Kersebaum KC, Skjelvåg AO, Seguin B, Peltonen-sainio P, Rossi F, Kozyra J, Micale F.
599 2011. Impacts and adaptation of European crop production systems to climate change. Eur. J. Agron 34(2):96–
600 112. https://doi.org/10.1016/j.eja.2010.11.003
601 Peltonen-Sainio P. 2012. Crop production in a northern climate. Building resilience for adaptation to climate
602 change in the agriculture sector. Proceedings of a Joint FAO/OECD workshop, 183−216.
603 Parent B., Leclere M., Lacube S., Semenov M.A., Welcker C., Martre P., Tardieu F. Maize yields over Europe
604 may increase in spite of climate change, with an appropriate use of the genetic variability of flowering time.
605 2018. Proceedings of the National Academy of Sciences, 115 (42), 10642−10647.
606 DOI: 10.1073/pnas.1720716115
607 Prein A. F., and Gobiet, A. 2017. Impacts of uncertainties in Europeangridded precipitation observations on
608 regional climate analysis. International Journal of Climatology, 37: 305–327. doi.org/10.1002/joc.4706
609 Ramirez-Cabral N.Y.Z., Kumar L., Shabani F. 2017. Global alterations in areas of suitability for maize production
610 from climate change and using a mechanistic species distribution model (CLIMEX). Scientific Reports, 7,
611 2092. doi.org/10.1038/s41598-017-05804-0
612 Ray DK, West PC, Clark M, Gerber JS, Prishchepov AV, Chatterjee S. 2019. Climate change has likely already
613 affected global food production. PLoS ONE 14 (5): e0217148. https:// doi.org/10.1371/journal.pone.0217148
614 Reichstein M., Bahn M., Ciais P., Frank D., Mahecha M.D., Seneviratne S.I., Zscheischler J., Beer C., Buchmann
615 N., Frank D.C., Papale D., Rammig A., Smith P., Thonicke K., van der Velde M., Vicca S., Walz A.,
616 Wattenbach. 2013. Climate extremes and the carbon cycle. Nature, 500, 287−295. doi: 10.1038/nature12350.

Rennie, S., et al. 2021. A climate service for ecologists: sharing pre-processed EURO-CORDEX regional climate scenario data using the eLTER Information System.Earth System Science Data, 13 (2): 631-644. doi.org/10.5194/essd-13-631-2021

Ritchie SW, Hanway JJ, Benson GO (1986) How a corn plant develops. Spec. Rep. 48.1owa State Univ. Coop. Ext. Serv, Ames, Iowa.

Riva-Roveda L., Escale B., Giauffret C., Périlleux C. 2016. Maize plants can enter a standby mode to cope with chilling stress. BMC Plant Biology, 16:212. doi: 10.1186/s12870-016-0909-y

Rötter R.P., Appiah M., Fichtler E., Kersebaum K.C., Trnka M., Hoffmann M.P.2018. Linking modelling and experimentation to better capture crops impacts of agroclimatic extremes − A review. Field Crops Research, 221, 142−156. doi.org/10.1016/j.fcr.2018.02.023

Sah R.P., Chakraborty M., Prasad K., Pandit M., Tudu V.K., Chakravarty M.K., Narayan S. C., Rana M., Moharana D. 2020. Impact of water deficit stress in maize: Phenology and yield components. Scientific Reports, 10: 2944. doi.org/10.1038/s41598-020-59689-7

Sanghera G.S., Wani S.H., Hussain W, Singh N.B. 2011. Engineering Cold Stress Tolerance in Crop Plants. Current Genomics, 12 (1): 30−43. doi: 10.2174/138920211794520178

Schaldach R., Koch J., Aus der Beek T., Kynast E., Flörke M. 2012. Current and future irrigation water requirements in pan-Europe: An integrated analysis of socio-economic and climate scenarios. Global and Planetary Change, 94−95: 33−45. doi.org/10.1016/j.gloplacha.2012.06.004

Schils R., Olesen J.E., Kersebaum K., Rijk B., Oberforster M., Kalyada V., et al. 2018. Cereal yield gaps across Europe. European yield gaps across Europe. European Journal of Agronomy, 101: 109−120. doi.org/10.1016/j.eja.2018.09.003

Schindler U., Durner W., von Unold G., Mueller L. 2010. Evaporation method for measuring unsaturated hydraulic properties of soils: Extending the measurement range. Soil Sci Soc Am J 74(4):1071–1083. doi.org/10.2136/sssaj2008.0358

Schleussner C.F., Deryng D., Müller C., Elliot J., Saeed F., Folberth C., Liu W., Wang X., Pugh T. A. M., Thiery W. 2018. Crop productivity changes in 1.5 °C and 2 °C worlds under climate sensitivity uncertainty. Environmental Research Letter, 13 (6). doi.org/10.1088/1748-9326/aab63b

Ureta C., González E. J., Espinosa A., Trueba A., Piñeyro-Nelson A., Álvarez-Buylla E.R. 2020. Maize yield in Mexico under climate change. Agricultural Systems, 177. doi.org/10.1016/j.agsy.2019.102697

Vogel E., Donat M.D., Alexander L., Meinshausen M., Ray D.K., Karoly D., Meinshausen N., Frieler K. 2019. The effects of climate extremes on global agricultural yields. Environmental Research Letters, 14 (5), 054010. https://doi.org/10.1088/1748-9326/ab154b

Webber, H., Hoffmann, M., Rezaei, E.E. 2020. Crop models as tools for agroclimatology. Agroclimatol. Link. Agric. Clim. 60, 519–546. doi.org/10.2134/agronmonogr60.2016.0025

WRB. 2014. World Reference Base for Soil Resources 2014. International soil classification system for naming soils and creating legends for soil maps. World Soil Resources Reports No. 106. FAO, Rome.

Wiréhn L. 2018. Nordic agriculture under climate change: A systematic review of challenges, opportunities and adaptation strategies for crop production. Land Use Policy, 77, 63−74. doi.org/10.1016/j.landusepol.2018.04.059

Xiao D., Liu D.L., Wang B., Feng P., Bai H., Tang J. 2020. Climate change impact on yields and water use of wheat and maize in the North China Plain under future climate change scenarios. Agricultural Water Management, 238. doi.org/10.1016/j.agwat.2020.106238

Zhang H., Han M., Comas L.H., DeJonge K.C., Gleason M.S., Trout T.J., Ma L. 2019. Response of Maize Yield Components to Growth Stage-Based Deficit Irrigation. Climatology and water management, 111 (6): 3244−3252. doi.org/10.2134/agronj2019.03.0214

Žydelis R., Weihermüller L., Herbst M., Klosterhalfen A., Lazauskas S. 2018. A model study on the effect of water and cold stress on maize development under nemoral climate. Agricultural and Forest Meteorology, 263: 169−179. doi.org/10.1016/j.agrformet.2018.08.011

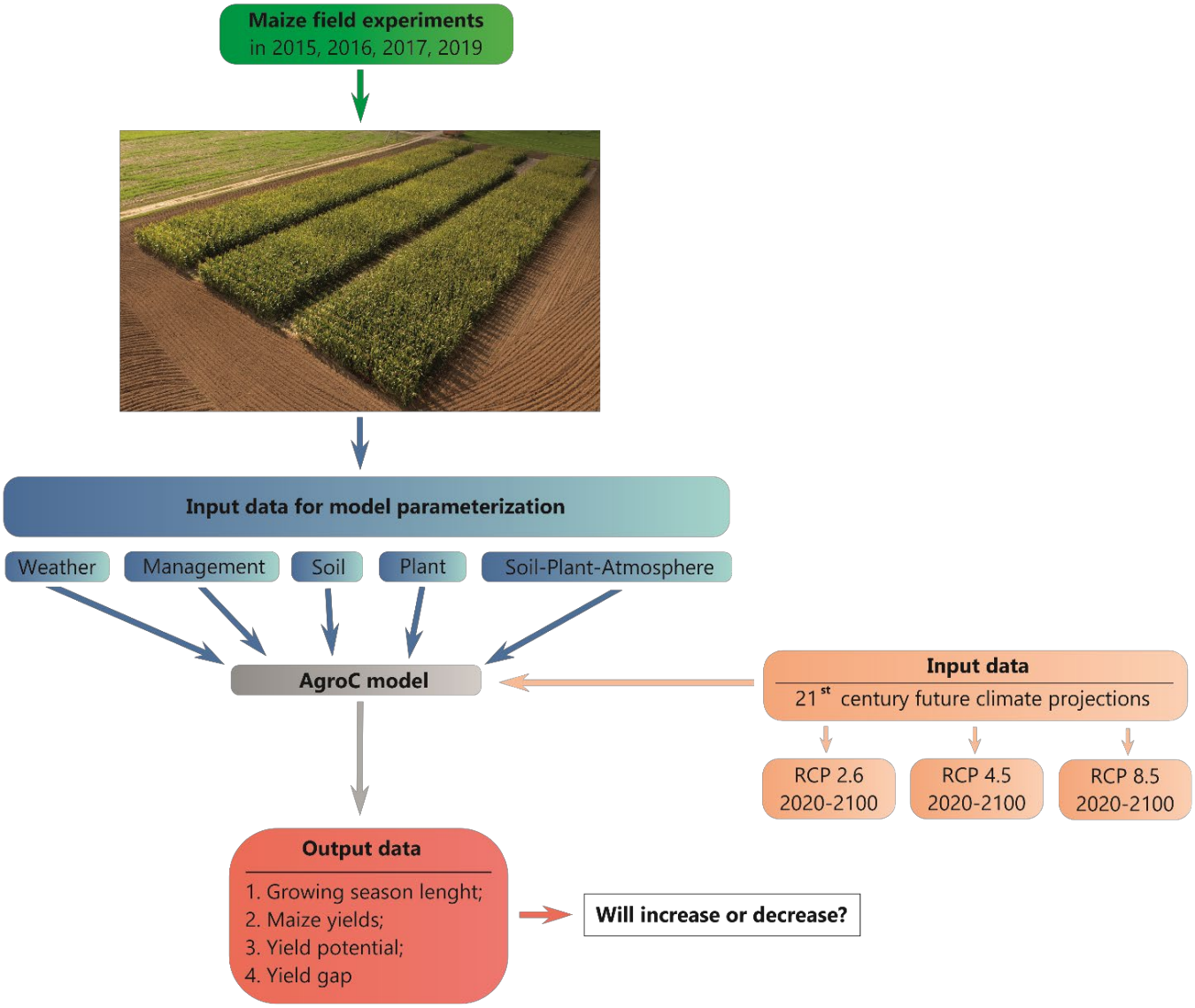

669
670
671 **Graphical abstract**
672
673
674

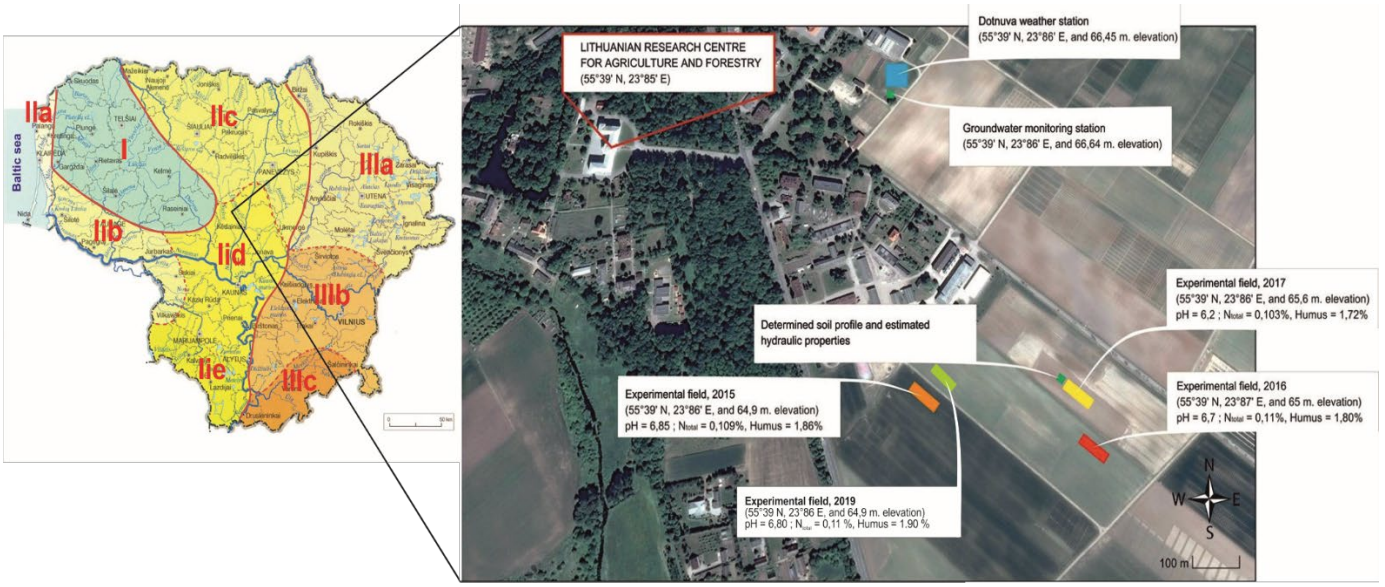

Figure 1. Lithuanian agroclimatic zones (on the left) and geographical positions of the studied maize experimental fields for the years 2015−2017 and 2019 (on the right). The numbers (I, II, III) and the letters (a, b, c, d, e) denote districts and subdistricts of agroclimatic zones, respectively.

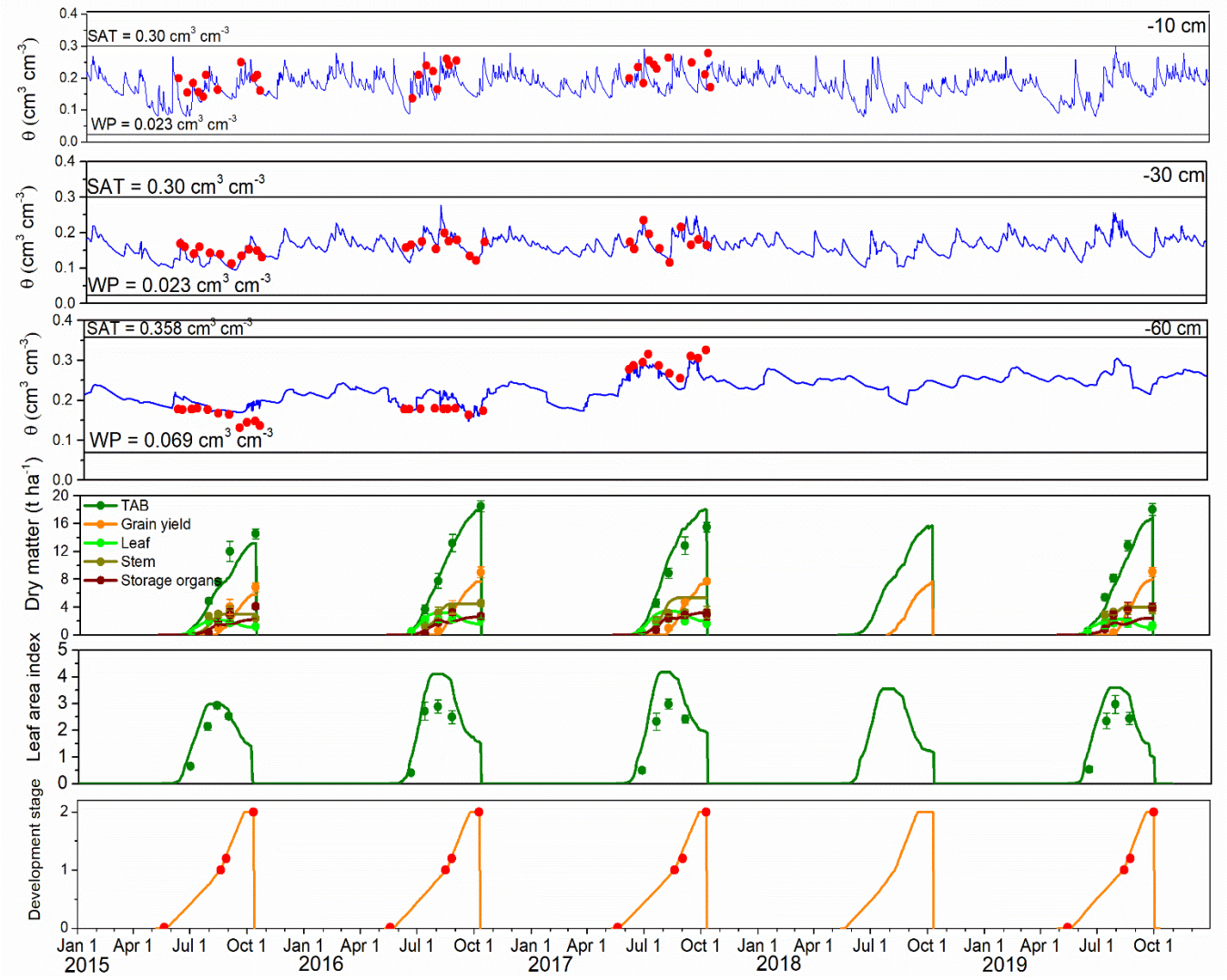

Figure 2. Comparison between the observed (dots, error bars) and simulated (lines) volumetric soil water content (θ) at three depths (0–10, 30 and 60 cm), total above-ground biomass (TAB), grain yield, leaf, stem and storage organ weights, dry matter, leaf area index and development stages (DVS) for the calibration (2016–2016) and validation (2017 and 2019) periods for rainfed maize in Akademija. SAT is the water content at full saturation and PWP is the water content at permanent wilting point, calculated from the retention function measured in the lab (see Table 2).

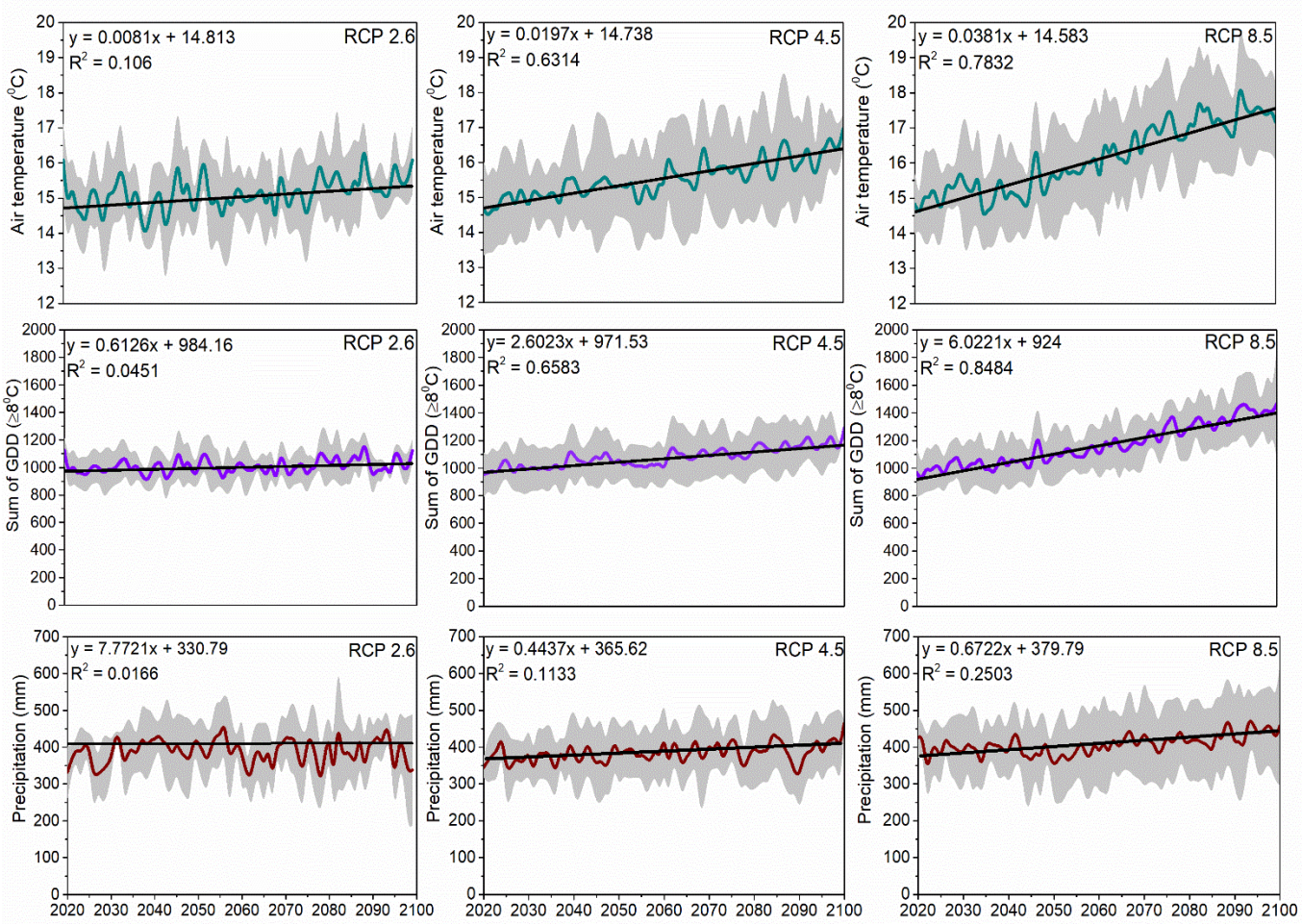

Figure 3. Projected seasonal mean air temperature, the sum of growing degree days (GDD) and precipitation under different climate change scenarios (RCP2.6, RCP4.5 and RCP8.5). The coloured lines show the mean values, while the filled areas show the standard deviation and the black line is the linear trend.

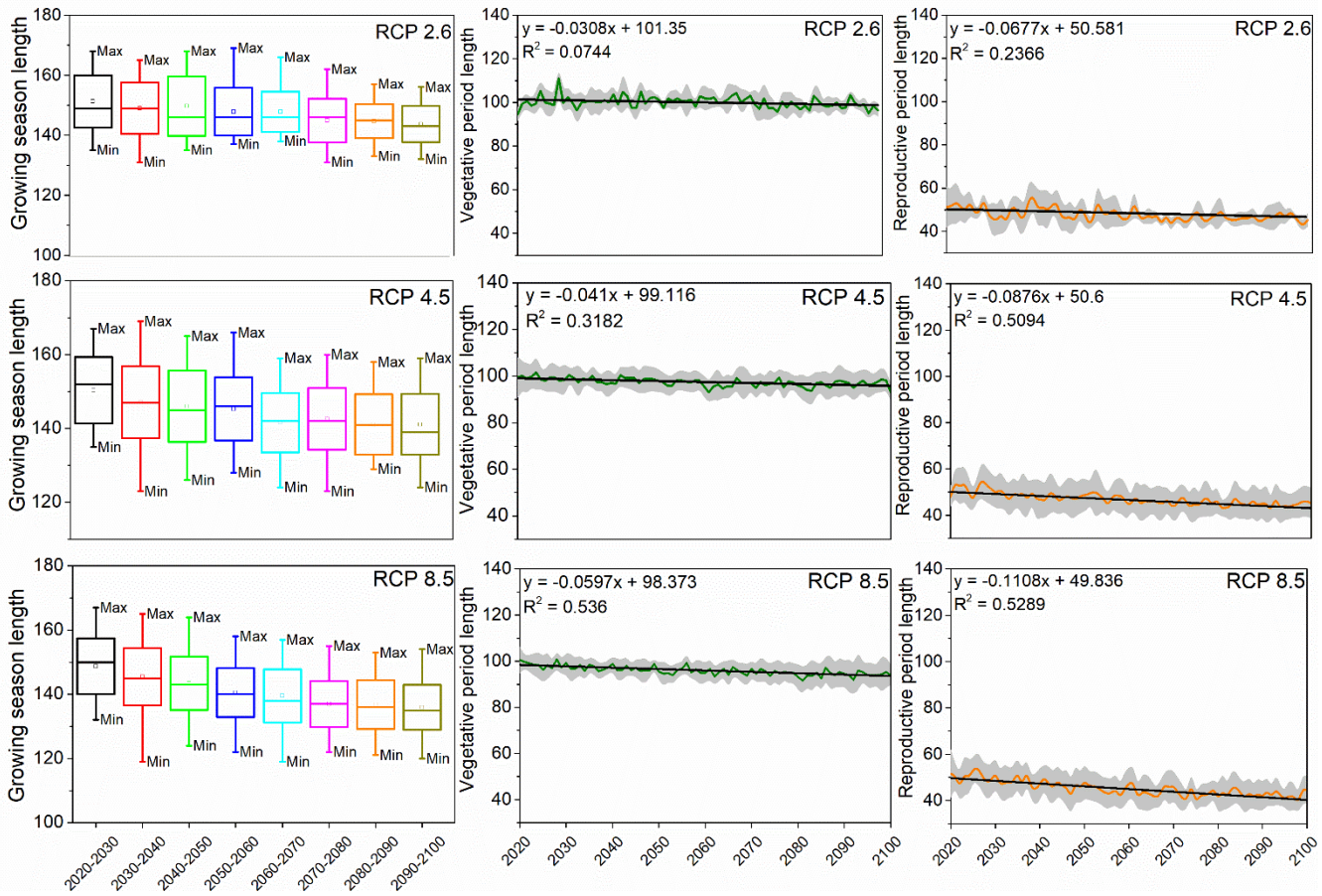

Figure 4. Projected changes in decadal maize growing season length (left), vegetative growing season length (middle) and reproductive growing season length (right) for the time period 2020−2100 under RCP2.6, RCP4.5 and RCP8.5. Each boxplot presents the different downscaling of the individual GCMs. Box boundaries indicate the 25th and 75th percentiles, whiskers below and above indicate minimum and maximum values. Lines and rectangles within each box indicate median and mean, respectively. The coloured lines (figures in middle and right) show the mean values, while the filled areas show the standard deviation and the black line is the linear trend.

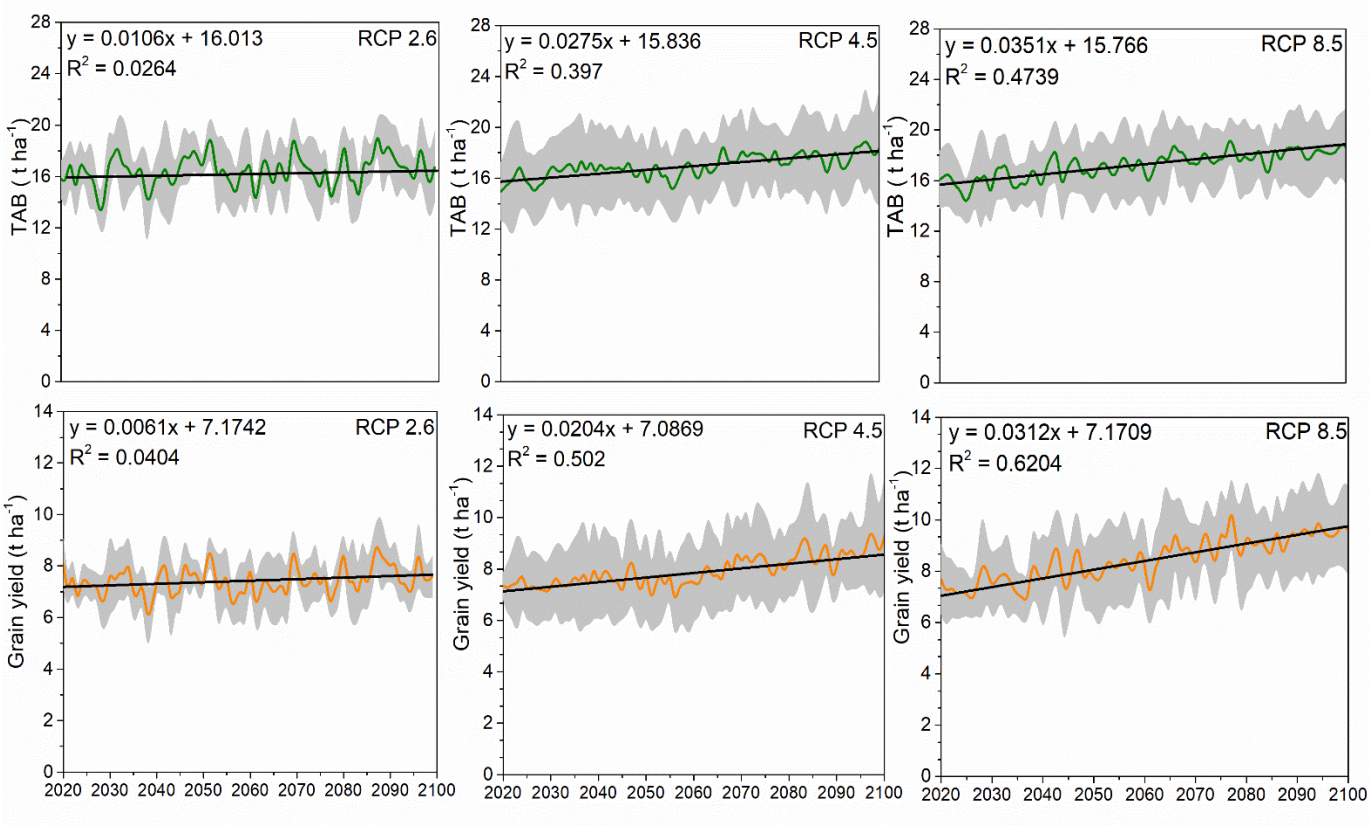

Figure 5. Predicted total above-ground biomass (TAB) and grain yield as dry matter for the long-term future climate change (2020−2100) under RCP2.6, RCP4.5 and RCP8.5. The coloured lines show the mean values, while the filled areas show the standard deviation and the black line is the linear trend.

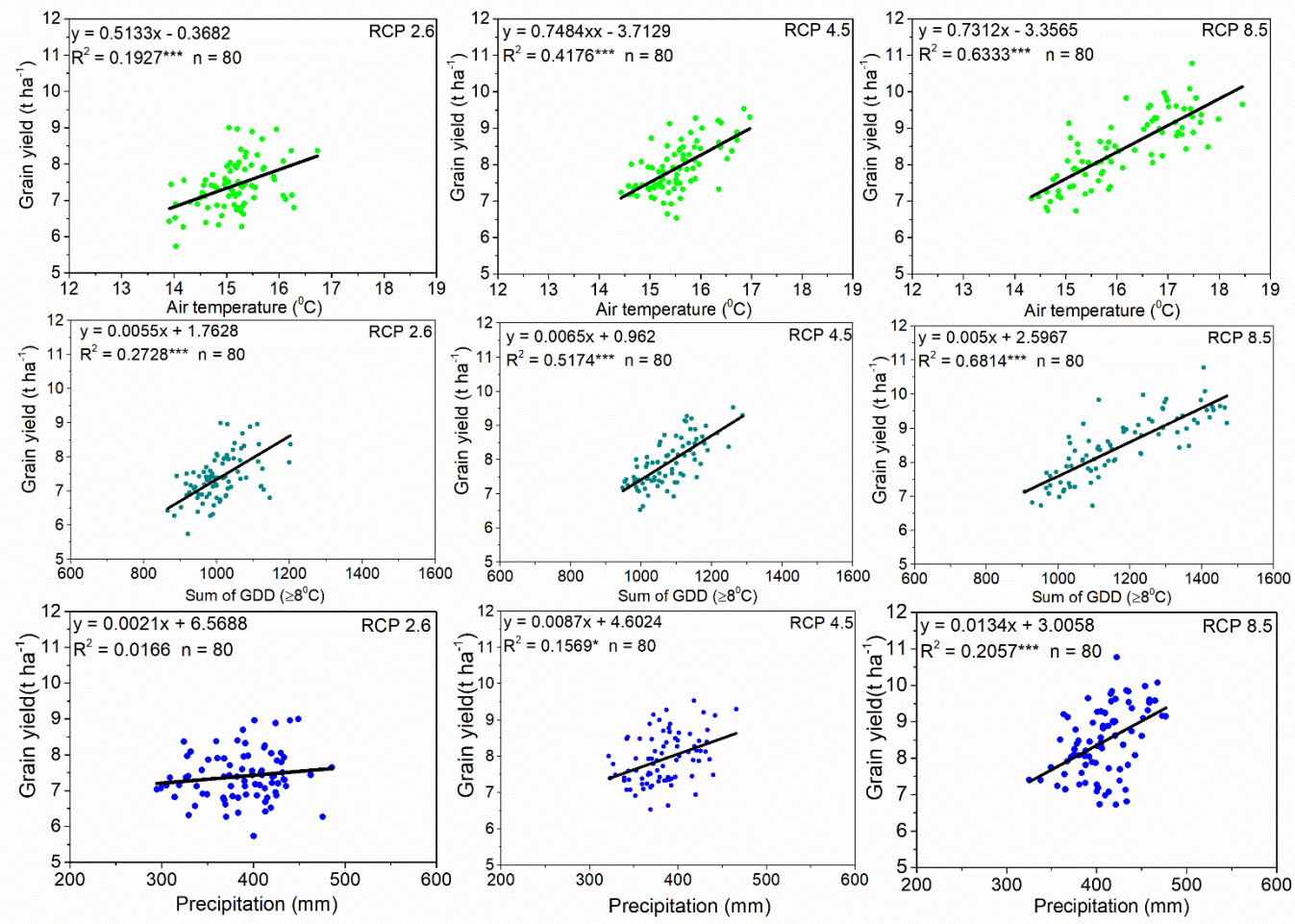

Figure 6. Linear regression between mean air temperature, sum of growing degree days (GDD) and precipitation over the growing season and dry matter grain yield for RCP2.6, RCP4.5 and RCP8.5**.** * $p < 0.05$, ** $p < 0.01$, *** $p < 0.001$

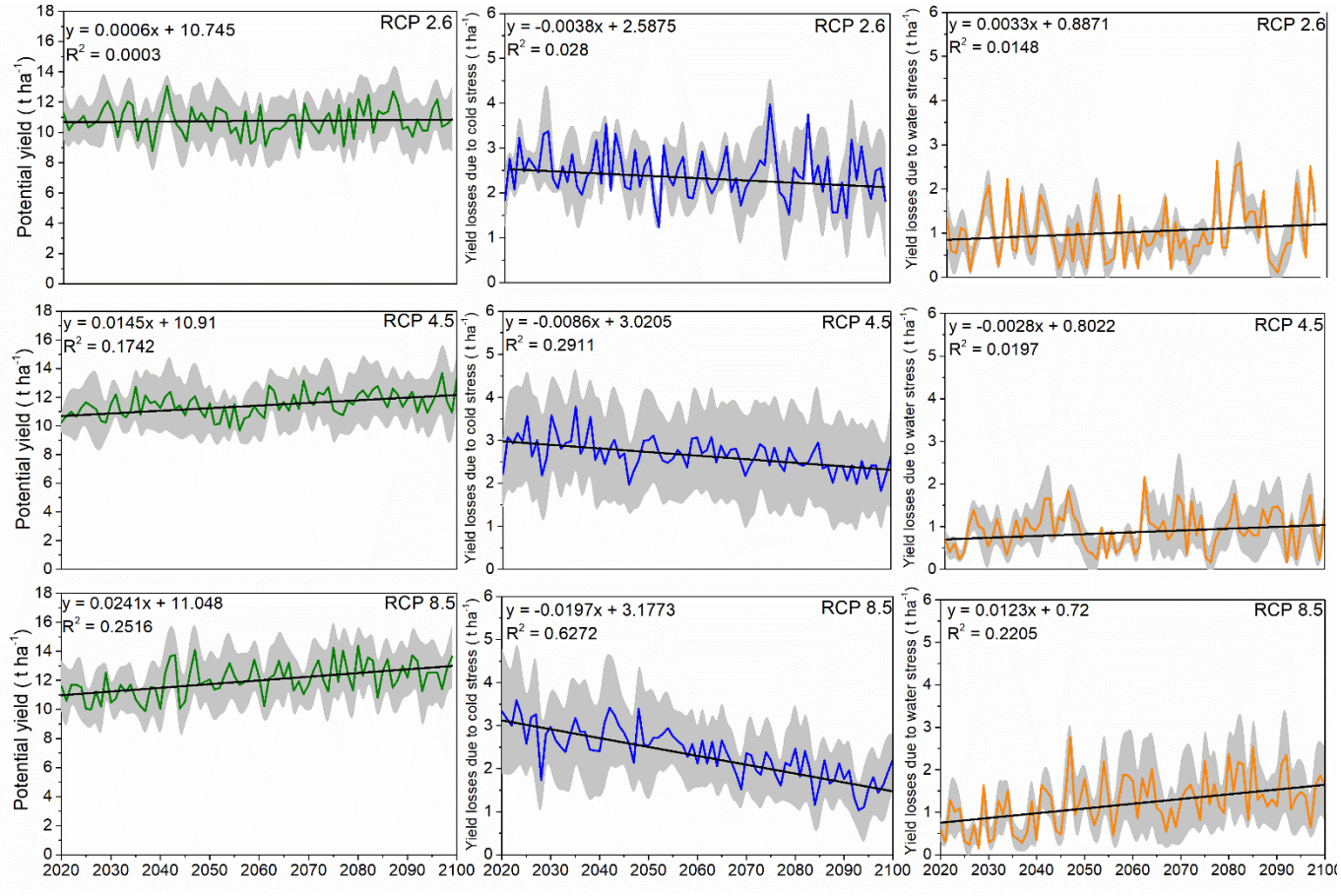

Figure 7. Predicted potential yields (t ha^{-1} at dry matter) and yield gap (t ha^{-1} of yield potential) of rainfed maize for the time period 2020−2100 under RCP2.6, RCP4.5 and RCP8.5. The coloured lines show the mean values, while the filled areas show the standard deviation and the black line is the linear trend.

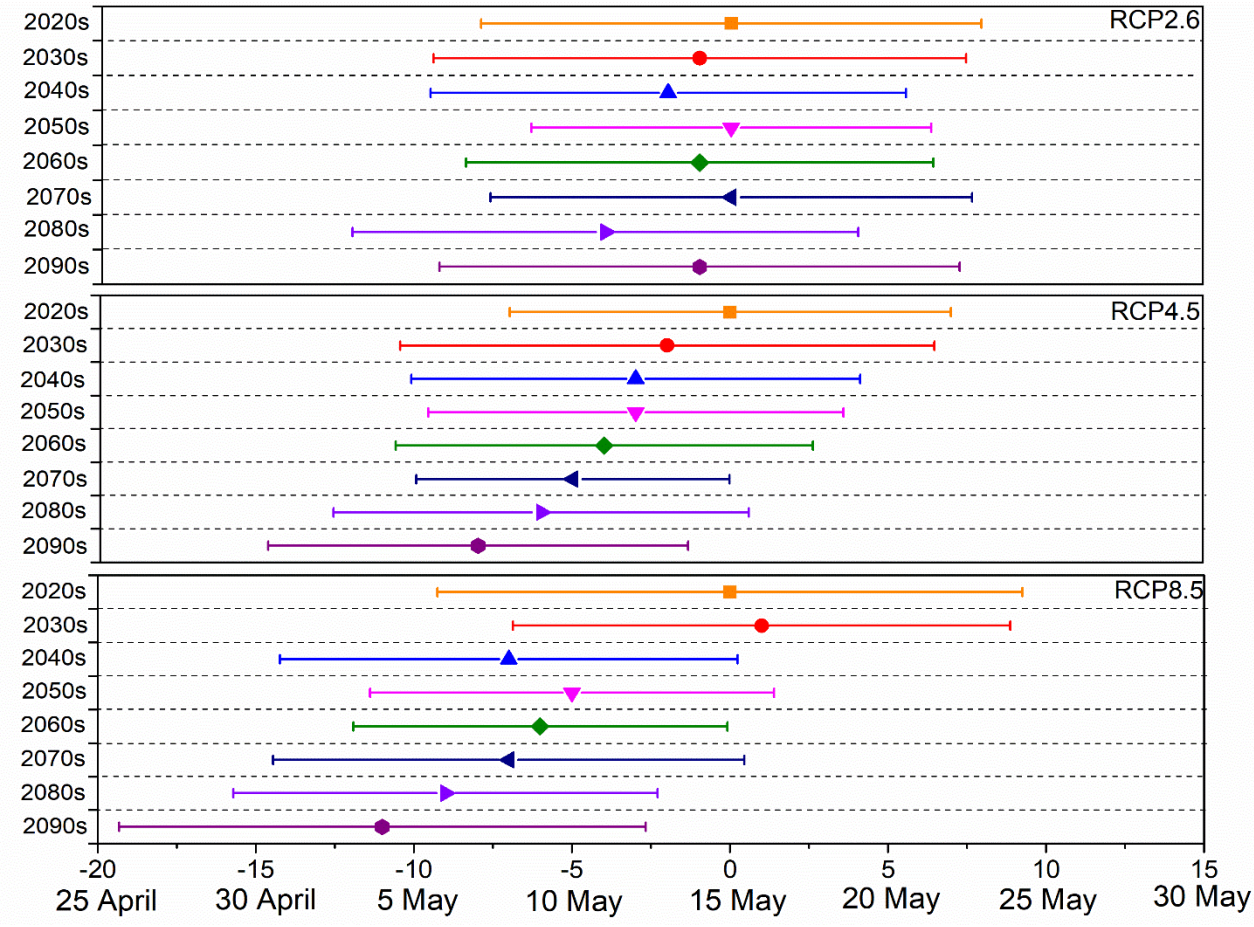

Supplementary Figure 1. Maize sowing date shifts projected for future decades under different RCP scenarios. The coloured symbols show the mean values, while the horizontal lines show the standard deviation.

771

772 **Table 1.** Soil characteristics of the topsoil layer (0−20 cm) and field management data.

	2015	2016	2017	2019
Soil pH_{KCl} (1 N KCl extraction)	6.85	6.70	6.20	6.80
Soil P_2O_5 (mg kg^{-1}) (Egner-Riehm-Domingo (A-L))	154	129	85	85
Soil K_2O (mg kg^{-1}) (Egner-Riehm-Domingo (A-L))	138	140	154	134
Soil humus (%) (Tjurin)	1.86	1.80	1.72	1.90
Soil N total (%) (Kjeldahl)	0.109	0.11	0.103	0.11
NO_3^- −N (0−30 cm; mg kg^{-1})	8.4±0.9	9.4±2.3	4.2±1.2	7.8±0.8
NH_4^+ −N (0−30 cm; mg kg^{-1})	1.8±0.5	3.7±1.4	2.5±0.1	2.4±0.3
NO_3^- −N (31−60 cm; mg kg^{-1})	4.3±0.6	4.9±0.7	2.2±0.3	3.1±0.4
NH_4^+ −N (0−30 cm; mg kg^{-1})	1.2±0.3	2.7±1.1	1.8±0.4	1.3±0.3
Previous crop	spring rape	spring rape	winter wheat	winter wheat
Maize sowing date	8 May	10 May	10 May	29 April
Maize harvest	12 October	10 October	10 October	1 October

773
774

775 **Table 2.** Soil horizons, texture, soil water content (SWC), permanent wilting point (PWP), field capacity (FC), saturation
776 (SAT), total available water (TAW) and saturated hydraulic conductivity (K_{sat}) of the field experiments.

Horizon description	Particle size (%)			Textural class	Bulk density (g cm^{-3})	SWC (cm^3 cm^{-3}) at			TAW (cm^3 cm^{-3})	K_{sat} (cm day^{-1})
	Sand	Silt	Clay			PWP	FC	SAT		
Ap[1] (0–0.30 m)	55	31.9	13.1	Sandy loam	1.81	0.023	0.289	0.300	0.277	0.6
E[2] (0.30–0.60 m)	70.4	23.4	6.2	Sandy loam	1.70	0.069	0.354	0.358	0.289	2.2
Bt[3] (0.60–0.80 m)	35	35.7	29.3	Clay loam	1.73	0.122	0.317	0.342	0.220	6.1
B[4] (0.80–1.10 m)	57.5	22.6	19.9	Sandy loam	1.68	0.083	0.343	0.351	0.268	62.0
Ck[5] (1.10–1.55 m)	54.4	31.6	14	Sandy loam	1.96	0.062	0.234	0.245	0.183	3.2

777 [1]: mineral surface horizon with an accumulation of humified organic matter.

778 [2]: mineral horizon in which the main feature is loss of silicate clay.

779 [3]: mineral illuvial horizon with accumulation of silicate clay.

780 [4]: mineral illuvial horizon.

781 [5]: initial horizon with accumulation of paedogenic carbonates.

782

783

784

785

Table 3. Statistical values between the simulated vs. measured data for the calibration (2015−2016) and the validation (2017, 2019) periods for rainfed maize at Akademija.

Parameters	R^2				RMSE			
	2015	2016	2017	2019	2015	2016	2017	2019
SWC at 10 cm (cm^3 cm^{-3})	0.43	0.58	0.49	–	0.030	0.048	0.051	–
SWC at 30 cm (cm^3 cm^{-3})	0.61	0.58	0.70	–	0.014	0.019	0.021	–
SWC at 60 cm (cm^3 cm^{-3})	0.35	0.65	0.46	–	0.029	0.026	0.032	–
TAB (t ha^{-1})	0.96	0.99	0.99	0.97	0.99	0.40	1.02	1.28
Leaf biomass (t ha^{-1})	0.91	0.96	0.94	0.88	0.41	0.57	0.86	0.63
Stem biomass (t ha^{-1})	0.82	0.94	0.91	0.75	0.67	0.64	0.27	0.85
Storage organ biomass (t ha^{-1})	0.85	0.78	0.97	0.92	1.08	0.57	0.86	1.23
Grain yield (t ha^{-1})	0.97	0.99	0.99	0.96	0.83	0.93	0.48	0.75
LAI	0.96	0.97	0.86	0.97	0.31	0.95	1.16	0.83

TAB = total above-ground biomass; LAI = leaf area index; SWC = soil water content

809

810 **Supplementary Table 1.** Main AgroC parameters used in the simulation of maize growth at Akademija, Lithuania.
811 GDD = sum of growing degree days, LAI = leaf area index, DVS = development stage

Parameters	Value	Units or symbol meaning	Remarks
Base temperature	8	°C	Conservative
Start temperature for plant growth	80	Sum of GDD	Calibrated
Specific leaf area of new leaves	0.004	ha leaf kg^{-1} dry matter	Calibrated
Potential CO_2 assimilation rate of a unit leaf area for light saturation	58	kg CO_2 ha^{-1} leaf h^{-1}	Calibrated
Initial light use efficiency	0.68	(kg CO_2 ha^{-1} leaf h^{-1})(J m^{-2} s^{-1})$^{-1}$	Calibrated
Maximal rooting depth	1.0	m	Calibrated
Number of seedlings per area	7	m^{-2}	Measured
Leaf area of one seedling	0.000669	m^{-2} per seedling	Calibrated
Critical LAI for leaf death due to self-shading	4	ha ha^{-1}	Conservative
DVS against reduction factor of the maximal light assimilation rate	0 1.0 1.3 1.0 1.6 1.0 2 0.3	DVS = 1.0: Tasseling; DVS = 2.0: Physiological maturity	Calibrated
Daily average daytime temperature against reduction factor of the maximal light assimilation rate	-10 0.01 9 0.05 16 0.80 18 0.94 20 1.00 30 0.75	Temperature in °C	Calibrated
Daily average temperature against development rate, if DVS < 1	-10 0.0000 0 0.0000 8 0.0015 10 0.0090 15 0.0109 20 0.0116 25 0.0159 30 0.0163 35 0.0316 40 0.0367		Calibrated
Daily average temperature against development rate, if DVS > 1	-10 0.0000 0 0.0000 8 0.0004 10 0.0226 15 0.0259 20 0.0288 25 0.0305 30 0.0324		Calibrated

	35	0.0336	
	40	0.0352	
DVS against fraction of dry matter allocated to the shoot	0.0	0.30	Calibrated
	0.1	0.55	
	0.2	0.60	
	0.4	0.66	
	0.5	0.69	
	0.7	0.85	
	0.9	1.00	
	1.0	1.00	
	2.0	1.00	
DVS against fraction of dry matter of the above ground biomass allocated to the leaves	0.0	0.70	Calibrated
	0.25	0.90	
	0.8	0.20	
	0.9	0.00	
DVS against fraction of dry matter of the above ground biomass allocated to the stem	0.0	0.00	Calibrated
	0.25	0.00	
	0.8	0.65	
	0.9	0.45	
	1.1	0.00	
DVS against fraction of dry matter of the above ground biomass allocated to the cob	0.0	0.00	Calibrated
	0.8	0.00	
	0.9	0.75	
	1.1	0.90	
	1.4	0.80	
	2.0	1.00	

Supplementary Table 2. List of general circulation models (GCM) and regional climate models (RCM) under RCP2.6, RCP4.5 and RCP8.5 future climate scenarios used in this study.

GCM	Institute ID	Country	RCM	Institute ID	Country
		RCP2.6			
MOHC-HadGEM2-ES	MOHC	UK	KNMI-RACMO22E	KNMI	Netherlands
MOHC-HadGEM2-ES	MOHC	UK	SMHI-RCA4	SMHI	Sweden
MPI-M-MPI-ESM-LR	MPI-M	Germany	MPI-CSC-REMO2009	MPI	Germany
MPI-M-MPI-ESM-LR	MPI-M	Germany	SMHI-RCA4	SMHI	Sweden
		RCP4.6			
CNRM-CERFACS-CNRM-CM5	CNRM	France	SMHI-RCA4	SMHI	Sweden
ICHEC-EC-EARTH	ICHEC	Ireland	KNMI-RACMO22E	KNMI	Netherlands
IPSL-IPSL-CM5A-MR	IPSL	France	IPSL-INERIS-WRF331F	IPSL	France
IPSL-IPSL-CM5A-MR	IPSL	France	SMHI-RCA4	SMHI	Sweden
MPI-M-MPI-ESM-LR	MPI-M	Germany	CLMcom-CCLM4-8-17	CLMcom	–
MPI-M-MPI-ESM-LR	MPI-M	Germany	MPI-CSC-REMO2009	MPI	Germany
MPI-M-MPI-ESM-LR	MPI-M	Germany	SMHI-RCA4	SMHI	Sweden
NCC-NorESM1-M	NCC	Norway	DMI-HIRHAM5	DMI	Denmark
MOHC-HadGEM2-ES	MOHC	UK	KNMI-RACMO22E	KNMI	Netherlands
MOHC-HadGEM2-ES	MOHC	UK	SMHI-RCA4	SMHI	Sweden
		RCP8.5			
CNRM-CERFACS-CNRM-CM5	CNRM	France	SMHI-RCA4	SMHI	Sweden
ICHEC-EC-EARTH	ICHEC	Ireland	KNMI-RACMO22E	KNMI	Netherlands
IPSL-IPSL-CM5A-MR	IPSL	France	IPSL-INERIS-WRF331F	IPSL	France
IPSL-IPSL-CM5A-MR	IPSL	France	SMHI-RCA4	SMHI	Sweden
MOHC-HadGEM2-ES	MOHC	UK	KNMI-RACMO22E	KNMI	Netherlands
MOHC-HadGEM2-ES	MOHC	UK	SMHI-RCA4	SMHI	Sweden
MPI-M-MPI-ESM-LR	MPI-M	Germany	CLMcom-CCLM4-8-17	CLMcom	–
MPI-M-MPI-ESM-LR	MPI-M	Germany	MPI-CSC-REMO2009	MPI	Germany
MPI-M-MPI-ESM-LR	MPI-M	Germany	SMHI-RCA4	SMHI	Sweden
NCC-NorESM1-M	NCC	Norway	DMI-HIRHAM5	DMI	Denmark

IPSL = Institut Pierre Simon Laplace, CNRM = Centre National de Recherches Meteorologiques, DMI = Danish Meteorological Institute, KNMI = Royal Netherlands Meteorological Institute, SMHI = Swedish Meteorological and Hydrological Institute, Rossby Centre, MPI = Helmholtz Zentrum Geesthacht, Climate Service Centre, CLMcom = Climate Limited-area Modelling Community, MOHC = The Met Office Hadley Centre, MPI-M = The Max Planck Institute for Meteorology, ICHEC = Irish Centre for High End Computing, NCC = Norwegian Climate Centre